ELSEVIER

Palaeogeography, Palaeoclimatology, Palaeoecology 199 (2003) 107–127

PALAEO

www.elsevier.com/locate/palaeo

Late Maastrichtian paleoclimatic and paleoceanographic changes inferred from Sr/Ca ratio and stable isotopes

D. Stüben [a], U. Kramar [a,*], Z.A. Berner [a], M. Meudt [a], G. Keller [b], S. Abramovich [b], T. Adatte [c], U. Hambach [d], W. Stinnesbeck [e]

[a] *Institut für Mineralogie und Geochemie, Universität Karlsruhe, Kaiserstr. 12, 76128 Karlsruhe, Germany*
[b] *Department of Geosciences, Princeton University, Princeton, NJ 08544, USA*
[c] *Institute de Geologie, 11 Rue Emile Argand, 2007 Neuchâtel, Switzerland*
[d] *Geowissenschaften, Universität Bayreuth, D-95440 Bayreuth, Germany*
[e] *Geologisches Institut, Universität Karlsruhe, Postfach 6980, 76128 Karlsruhe, Germany*

Received 9 April 2002; accepted 4 June 2003

Abstract

Milankovitch-scale cycles can be recognized in high-resolution $\delta^{13}C$, $\delta^{18}O$, Sr/Ca, mineralogical, and magnetic susceptibility data in hemipelagic sediments that span the last 700 kyr of the Maastrichtian at Elles, Tunisia. Oxygen isotope data reveal three cool periods between 65.50 and 65.55 Ma (21.5–23.5 m), 65.26 and 65.33 Ma (8–11 m), and 65.04 and 65.12 Ma (1.5–4 m), and three warm periods between 65.33 and 65.38 Ma (12–16 m), 65.12 and 65.26 Ma (4–8 m), and 65.00 and 65.04 Ma (0–1.5 m). The cool periods are characterized by small surface-to-deep temperature gradients that reflect intensive mixing of the water column. The surface-to-deep Sr/Ca gradient generally correlates with the oscillating ΔT trend (temperature difference between surface and bottom waters). The carbon isotope composition of planktonic foraminifera indicates a continuous decrease in surface bioproductivity during Late Maastrichtian. Decreasing $\Delta^{13}C$ values (difference between the $\delta^{13}C$ values of surface and bottom dwelling foraminifera) and the carbon isotope ratios of the planktonic species at the onset of gradual warming at 65.50 Ma reflect a reduction in surface productivity as a result of decreased upwelling that accompanied global warming and possibly increased atmospheric pCO_2 related to Deccan Trap volcanism. Time series analysis applied to magnetic susceptibility, $\delta^{18}O$, and Sr/Ca data identifies the 20 kyr precession, 40 kyr obliquity, and 100 kyr eccentricity Milankovich cycles.

Keywords: Late Maastrichtian; stable isotopes; Sr/Ca; paleoclimate

1. Introduction

The Maastrichtian climate was characterized by long-term cooling followed by short-term warming (65.4–65.2 Ma) and rapid cooling near the end of the Maastrichtian (Shackleton et al., 1984; Zachos et al., 1985, 1986; Barrera and Huber, 1990; Stott and Kennett, 1990; Spicer and Corfield, 1992; D'Hondt and Lindinger, 1994; Barrera, 1994; Barrera et al., 1997; Li and Keller,

* Corresponding author.
E-mail addresses: doris.stueben@img.uni-karlsruhe.de (D. Stüben), utz.kramar@img.uni-karlsruhe.de (U. Kramar).

0031-0182/03/$ – see front matter © 2003 Elsevier B.V. All rights reserved.
doi:10.1016/S0031-0182(03)00499-1

1998a,b, 1999). Salinity fluctuations indicate that during the short-term global warming, high-latitude deep-water production was significantly reduced and warm saline deep waters, probably originating in the shallow middle- and low-latitude regions of the Tethys, flooded the ocean basins (Li and Keller, 1998b). The rapid warming may have been caused by increased CO_2 due to major Deccan Trap volcanism (Courtillot et al., 1996; Hoffmann et al., 2000) and possibly an impact event, as suggested by the recent discovery of glass spherule deposits in upper Maastrichtian sediments dated between 65.4 and 65.2 Ma (Stinnesbeck et al., 2001; Keller et al., 2002). Major faunal changes across latitudes associated with this greenhouse warming have been increasingly recognized by planktonic foraminiferal workers (Abramovich et al., 1998; Kucera and Malmgren, 1998; Li and Keller, 1998a,b; Olsson et al., 2001; McLeod et al., 2001).

Although these studies provide a tantalizing glimpse of the complexity of the climatic and environmental changes during the last 500 kyr of the Maastrichtian, their detailed nature is still unknown. This is largely because time control afforded by biostratigraphic and chronostratigraphic studies are typically on the order of hundreds of thousands of years, whereas oceanic processes operate on much shorter time scales of thousands of years or less. High-resolution sampling at the 5–10 cm level can improve the temporal resolution to several thousand years, as shown by Li and Keller (1998a) at the mid-latitude South Atlantic deep-sea DSDP Site 525A and by Abramovich and Keller (2002) for the Elles section in Tunisia. However, these paleontological studies also revealed that the rate of sedimentation was seven times higher in the low latitude Tethyan continental shelf at Elles, than in the open ocean Site 525A. High-resolution sample analysis of this expanded Tethys section thus provides a unique opportunity to recover a very detailed climatic and environmental record that is not available in open ocean sediments. This is the primary goal of this study.

In this study we evaluate the climatic and paleoceanographic history of the low-latitude Tethys continental shelf of Tunisia for the last 700 kyr of the Maastrichtian based on stable isotopes ($\delta^{13}C$ and $\delta^{18}O$), Sr/Ca ratios, magnetic susceptibility, and mineralogical studies. These extensive data sets provide information on paleoproductivity ($\delta^{13}C$), sea surface and bottom temperatures ($\delta^{18}O$ and Sr/Ca ratios), and sea level fluctuations (mineralogy and Sr/Ca ratios). Correlations among these various data sets and the Milankovitch cycles provide new insights into the Tethyan paleoenvironmental conditions during the terminal Maastrichtian.

2. Materials and methods

The Elles section is located 75 km southeast off the city of El Kef, Tunisia, and has been described by Li et al. (2000) and Abramovich and Keller (2002) (Fig. 1). Elles outcrops span a continuous succession from the Campanian to the Eocene. The uppermost Maastrichtian portion examined for this study consists of 30 m, spanning from chron 30N through 29R to the K/T boundary. Sediments comprise dark gray marls with some sandy to silty interlayers. Biostratigraphy is based on the planktonic foraminiferal zonation of Abramovich and Keller (2002) with zones CF1 and CF2 marking the last 300, respectively, 150 kyr of the Maastrichtian.

Two hundred and forty samples were analyzed at 20 cm intervals for this study. Sediments were disaggregated in water and washed through a 63 μm sieve until clean sample residues were obtained. From each sample about 15 specimens of the benthic foraminifer *Cibicidoides pseudoacuta* and 30 specimens of the planktonic foraminifer *Rugoglobigerina rugosa* (Fig. 2) were picked under the microscope for stable isotope analyses. The same species were also picked for Sr/Ca ratio analyses. Planktonic foraminiferal tests are well preserved, but show some recrystallization of the original test calcite. Stable carbon and oxygen isotope data were obtained using a fully automated preparation system (MultiCarb) connected on-line to an isotope ratio mass spectrometer (Optima, Micromass Limited UK). All carbon and oxygen isotope values are reported relative to

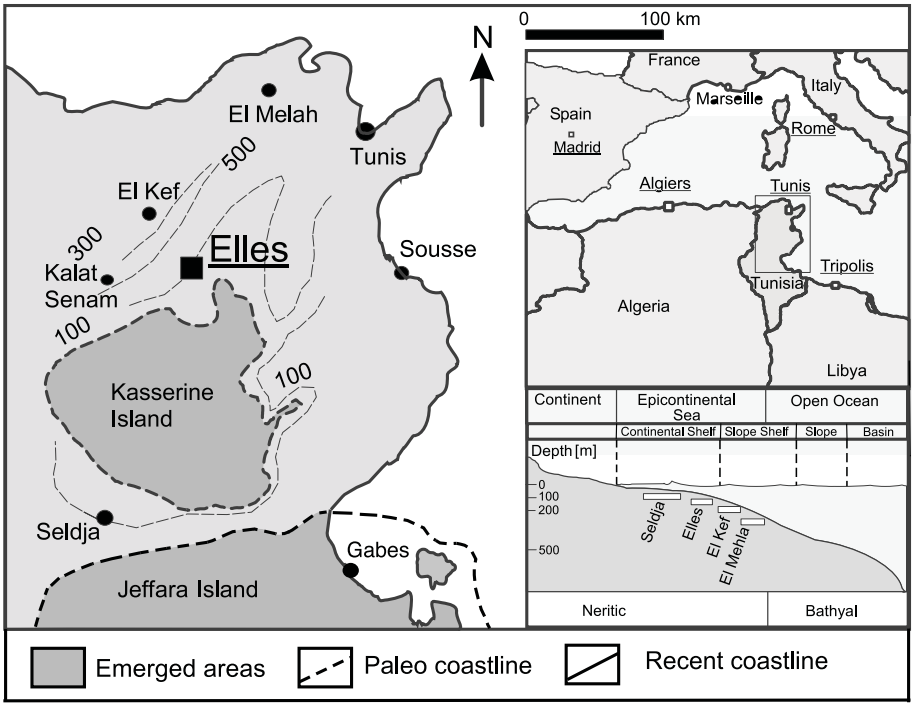

Fig. 1. Location of the Elles section in northwestern Tunisia 75 km SE of the city of El Kef (modified after Burollet, 1967 and Zaier et al., 1998), and schematic cross-section with paleogeographic positions of the Seldja, Elles, El Kef, and El Melah K–T sections.

the V-PDB standard. External reproducibility was better than 0.1 ‰ .

Strontium and Ca contents in foraminiferal tests were determined using total reflection X-ray fluorescence (Atomika EXTRA II) on one to six specimens (about 20 μg) with no visible Fe-oxide coatings or sediment infillings of chambers. Foraminifera were cleaned with bi-distilled water and transferred into PP-microcentrifuge tubes. One hundred μl of subboiled HNO_3, spiked with 0.2 ng Ga/μl as internal standard was used to digest the foraminiferal tests. The tubes were centrifuged at approximately 10 000 RCF to concentrate the sample and nitric acid in the cone-shaped bottom. Digestion was continued for 1 h in an ultrasonic bath, followed by a final centrifugation. Fifty μl of solution were transferred to a quartz sample carrier. After drying the samples were analyzed for 2000 s using a Mo tube (50 kV/38 mA) and filter, and a W tube, respectively. Strontium was normalized to Ca, with the actual sample weights calculated from the intensities of the Ga spikes.

For magnetic susceptibility determinations non-oriented samples with a spacing of 10 cm were taken from the 30 m interval below the K/T boundary. The rock was crushed, filled in plastic boxes and fixed with cotton wool. The susceptibility was measured with a KLY-2 Kappabridge (AGICO, Brno, CR) and normalized to its mass, because of the unknown in situ density of the sediment (the resulting unit is 10^{-6} SI/g). Assuming an average density of 2.4 g/cm^3 for the marls the given mass susceptibility values have to be multiplied by 24 in order to compare them to other data sets presented in original volume susceptibility (Hambach et al., 2002).

X-ray diffraction analyses of the whole rock were carried out for all the samples at the Geological Institute of the University of Neuchâtel. Whole rock mineralogy and clay mineral contents were measured with a SCINTAG XDS 2000 X-ray

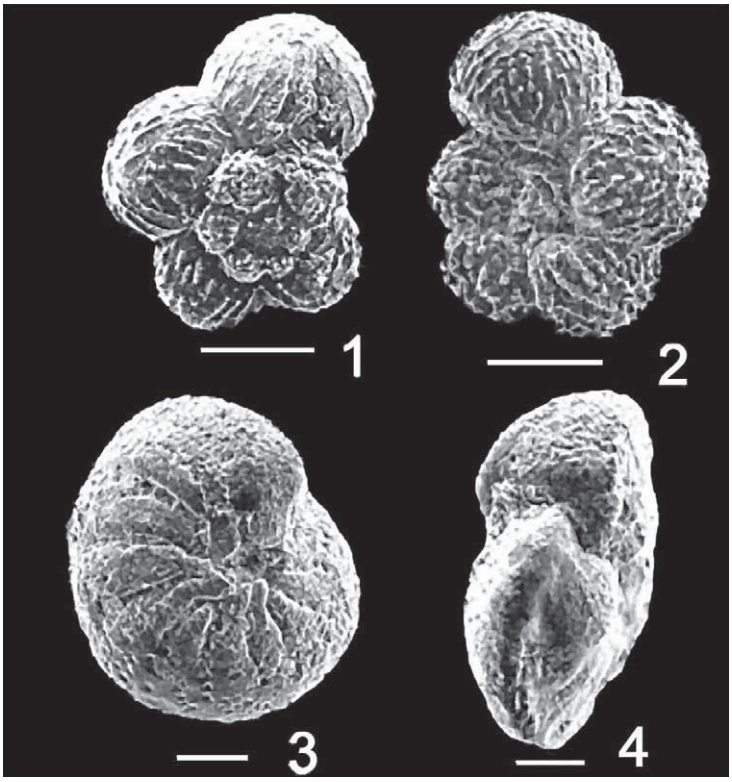

Fig. 2. SEM illustrations of foraminiferal species used for stable isotope analyses and Sr/Ca ratios. Scale bar represent 100 μm. (1, 2) *Rugoglobigerina rugosa*; (3, 4) *Cibicidoides pseudoacuta*.

powder diffractometer following the procedure described by Adatte et al. (1996).

3. Diagenesis

3.1. Diagenetic effects on stable isotopes

Oxygen isotope records of well-preserved monospecific foraminifera are currently the most accurate and useful means of climate change reconstruction. Although foraminifera are relatively well preserved at Elles, diagenesis seems to have altered the original signals, as indicated by scanning electron microscopy (SEM) images that reveal minor recrystallization and test overgrowth (Fig. 2), and some tests show calcite cement infillings. Similar diagenetic effects have been discussed by Mitchell et al. (1997), Pearson et al. (2001), Schrag et al. (1995), and Schrag (1999). Diagenetic effects at Elles are indicated by the overall low $\delta^{18}O$ values for planktonic and benthic foraminifera. A shift in the same direction can be due to burial diagenesis (Schrag et al., 1995), because recrystallization occurs at higher temperatures, and secondary carbonate with lower $\delta^{18}O$ values is formed in both planktonic and benthic species. Besides a shift toward lower $\delta^{18}O$ values due to the interaction with isotopically light meteoric waters, or equilibration at higher temperatures during burial, the effect of early diagenesis may also be a considerable factor (Schrag et al., 1995). Due to a high-temperature gradient between surface and bottom waters in low latitudes, early diagenetic recrystallization in the cool water environment of the ocean floor tends to shift primary oxygen isotope values of (mainly) planktonic foraminifera towards higher values and carbon isotopes towards lower values, indicating cooler sea surface temperatures and lower

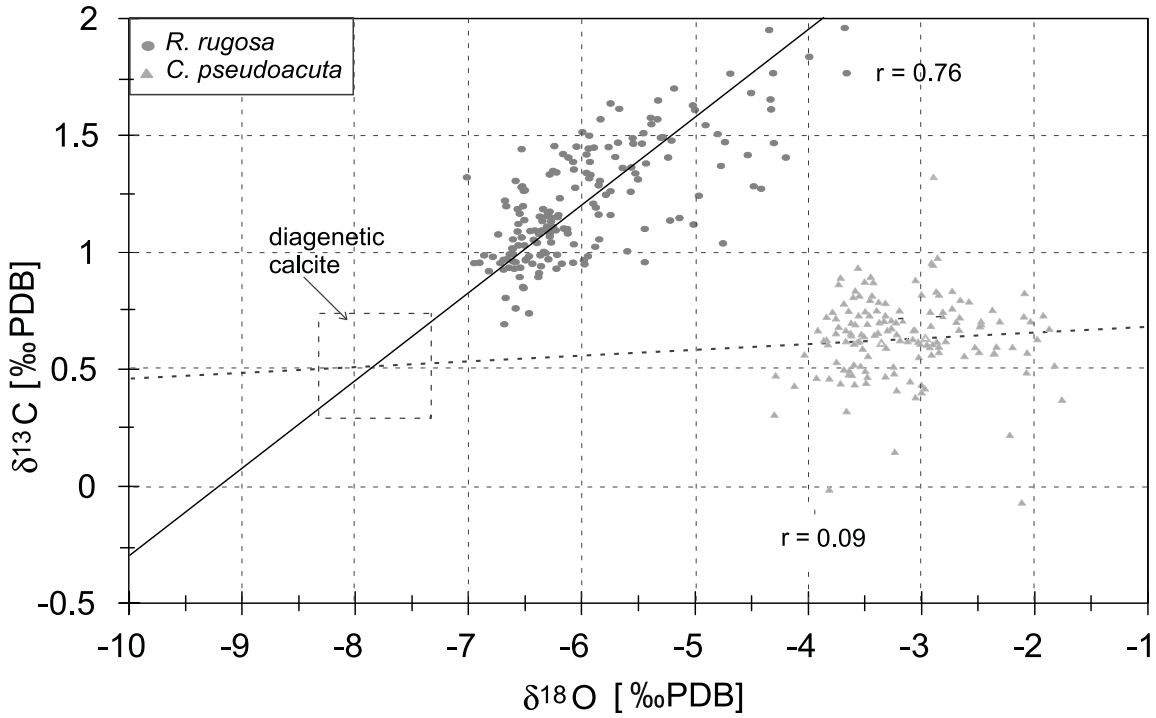

Fig. 3. Plot of $\delta^{18}O$ versus $\delta^{13}C$ of benthic and planktonic foraminifera from the Elles section. Note that the correlation between these data is weak for benthic ($r = 0.09$; $P = 0.259$) compared with planktonic foraminifera ($r = 0.76$; $P < 0.005$). Due to the small difference between $\delta^{13}C$ of diagenetic calcite and $\delta^{13}C$ of benthic foraminiferal tests the slope of the resulting mixing is small and the regression is masked by the non-diagenetic variation of the $\delta^{13}C$ values. The variation range of $\delta^{18}O$ for the benthic (~2.5‰) is only slightly lower than for the planktonic foraminiferal tests (~3‰), suggesting at most only minor differential diagenesis for pairs of benthic and planktonic foraminifera.

productivity compared to actual values (Schrag et al., 1992, 1995; Jenkyns et al., 1994; Mitchell et al., 1997; Sakai and Kano, 2001; Pearson et al., 2001). However, the shallow paleowater depth, and hence small temperature gradient between surface and bottom water, indicates that the effect of early recrystallization is presumably low and therefore has not to be taken into account at Elles. Today Elles is located at 36°N, but at the end of the Cretaceous the position of Elles was in low latitudes (close to the tropic of Cancer, Scotese and Sager, 1988) on the African continental shelf at an estimated paleowater depth of about ~150 m.

At Elles, the $\delta^{18}O/\delta^{13}C$ plot shows a significant positive correlation at the 99.95% level ($r = 0.76$; 175 sample pairs; error probability $P < 0.005$) for the planktonic foraminifer *Rugoglobigerina rugosa*, but no significant correlation ($r = 0.09$; 156 sample pairs; $P = 0.259$) for the benthic foraminifer *Cibicidoides pseudoacuta* (Fig. 3). This relationship is of particular interest to interpret the isotope records and discuss the possible alteration of primary isotope signals. There are several mechanisms which could lead to a correlation between $\delta^{18}O$ and $\delta^{13}C$:

(a) Based on experimental results, Spero et al. (1997) concluded that the covariance between $\delta^{13}C$ and $\delta^{18}O$ in foraminifera can be a consequence of changes in CO_3^{2-} content (i.e. in alkalinity) of seawater. However, the slopes of the regression lines in their study are much lower (0.29–0.33) than that observed in our data set (about 3.5), which rules out such an interpretation.

(b) Changes in salinity may also lead to covariance between the $\delta^{18}O$ and $\delta^{13}C$ (e.g. Khim and Park, 2000). The oxygen isotope composition of

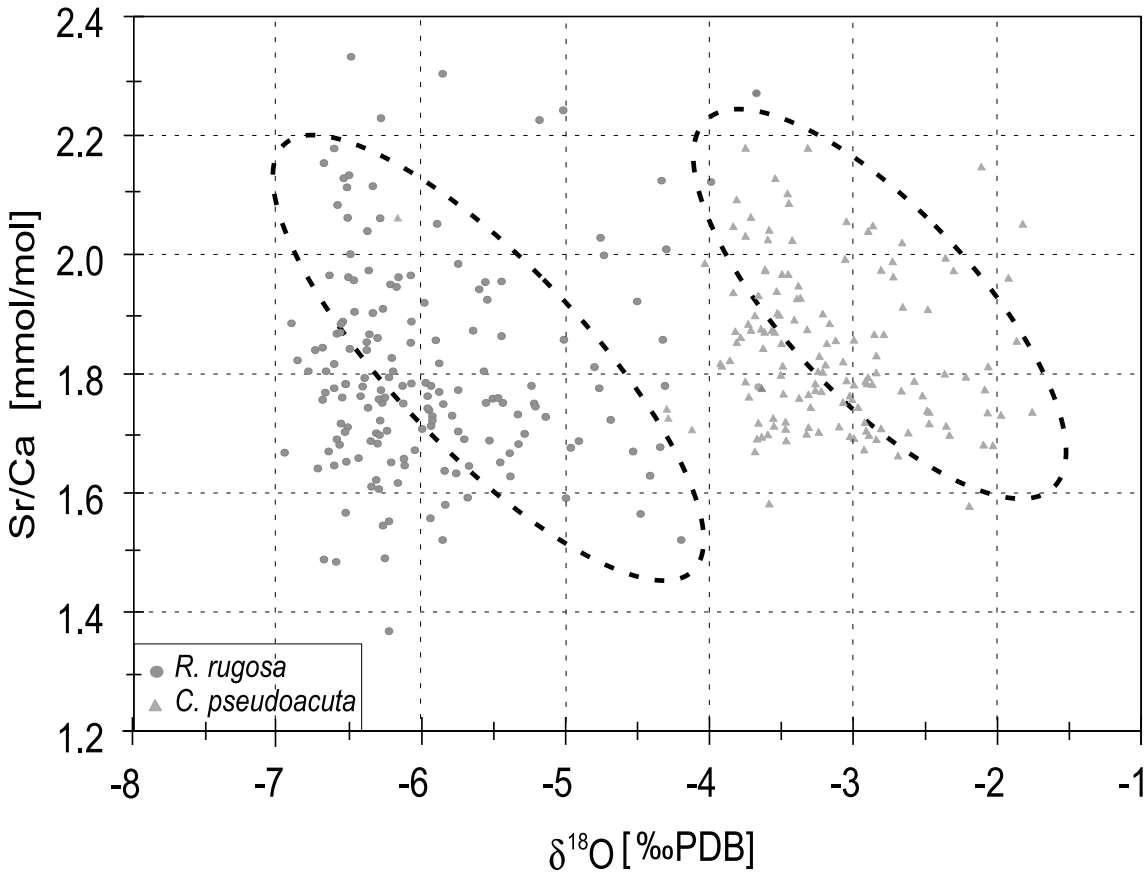

Fig. 4. Plot of $\delta^{18}O$ versus Sr/Ca ratio of benthic and planktonic foraminifera from the Elles section. The cluster of $\delta^{18}O$ and Sr/Ca suggests minor differential diagenetic alteration effects.

seawater is related to salinity either as a consequence of mixing between watermasses with different salinities and isotopic compositions, or of changes in the precipitation–evaporation cycle (e.g. Wolff et al., 1999; Pierre, 1999; Rohling and de Rijk, 1999). However, a correlation between $\delta^{18}O$ and $\delta^{13}C$ of foraminiferal carbonate is to be expected only if salinity changes are due to a higher input of continental run-off depleted in both ^{18}O and ^{13}C. Simple mass and isotope budget calculations (Martin and Letolle, 1979; Bédard et al., 1981), using rough end member estimates, indicate that the observed correlation is unlikely due to mixing. If we assume that late Cretaceous seawater differs in salinity and isotope composition by only a few ‰ from actual values (e.g. O'Neil, 1987), and that fresh water input (run-off/precipitation) for latitudes corresponding to the paleogeographic position of the study area (20°N) has typical values (salinity 1–2 psu; $\delta^{18}O$ about −5 to −7‰), then a shift in $\delta^{18}O$ of about 3–4‰ (as observed in our data set) would imply salinities between 7 and 20 psu. This corresponds to a fresh water contribution of about 45–80%. Similar conclusions may be drawn from the $\delta^{18}O$/salinity relationship in waters of modern tropical/subtropical oceans where the slope of the regression line is in the range of 0.18–0.25 (Schmidt, 1999; Wolff et al., 1999). Similar values (0.25–0.27) are reported for the Mediterranean basin, with a climate regime in which evaporation is in excess to fresh water input (Pierre, 1999).

Based on these data, the observed shift of 3–4‰ in $\delta^{18}O$ at Elles would correspond to a drop

in salinity of 12–22 psu. Such brackish conditions are ruled out by the presence of normal tropical to subtropical open ocean planktonic foraminiferal assemblages (Abramovich and Keller, 2002). In addition, the slope of the $\delta^{18}O/\delta^{13}C$ regression line is much higher than that reported for correlations relating on mixing (e.g. 0.53–0.57, Khim and Park, 2000). Nevertheless, it cannot be completely ruled out that simultaneous decreases in $\delta^{13}C$ and $\delta^{18}O$ of the Elles section are at least partly related to increased fresh water input and associated terrigenous debris. This may have been the case at the intervals around 7 and 22.5 m discussed below.

(c) Meteoric groundwaters are characterized by lower $\delta^{18}O$ ($\sim -10‰$ in low latitudes; Faure, 1986) and $\delta^{13}C$ values compared to seawater. Thus, in addition to a decrease in initial $\delta^{18}O$ values, varying degrees of cementation and/or recrystallization due to meteoric waters will also produce a correlation between the $\delta^{18}O$ and $\delta^{13}C$, and the samples therefore plot on a mixing line which links the initial $\delta^{18}O$ and $\delta^{13}C$ values of foraminifera with that of the diagenetic cement (Jenkyns et al., 1994; Mitchell et al., 1997; Sakai and Kano, 2001). In contrast, the addition of a constant amount of diagenetic calcite to each sample merely shifts all samples to more negative positions in Fig. 3, but will not induce a linear array. In this case, the oxygen isotope values cannot be interpreted in terms of absolute temperature, but the relative variations between them reflect primary signals, even if attenuated.

Fig. 3 shows that planktonic foraminifera at Elles narrowly cluster along a linear regression line, suggesting recrystallization, test overgrowth, and/or cement infillings. The greater variation in the $\delta^{18}O$ and $\delta^{13}C$ signals along the mixing line for planktonic species apparently suggests a higher degree of alteration or diagenetic infilling than in benthic foraminifera. It is therefore likely that at least the unusually low $\delta^{18}O$ values of the planktonic foraminifera are a result of diagenetic alteration due to interaction with meteoric waters, and/or recrystallization due to burial and associated thermal effects. The variability in isotopic values is likely a function of the ratio of original test carbonate to diagenetic carbonate in the form of chamber infilling. Based on the regression line between $\delta^{18}O$ and $\delta^{13}C$, the diagenetic cement in the Elles profile is estimated to average at ~ -8 to $-9‰$ for $\delta^{18}O$ and ~ 0.3 to $0.7‰$ for $\delta^{13}C$ (Fig. 3).

The benthic foraminiferal tests at Elles show no significant correlation between $\delta^{18}O$ and $\delta^{13}C$. However, the lack of correlation not compulsorily means that the benthic formaminifers are not affected by diagenetic overprint. Mitchell et al. (1997) observed that benthic foraminiferal tests are often less affected by diagenetic overprints than planktonic foraminiferal tests. Although this statement may be generally valid, it is very unlikely that in the scale of a single sample, planktonic and benthic formaminifers were affected to significantly different degrees by diagenesis. It is more likely that due to the small difference between $\delta^{13}C$ of the diagenetic calcite and $\delta^{13}C$ of the benthic foraminiferal tests the slope of the resulting mixing is small and the regression is masked by the non-diagenetic variation of the $\delta^{13}C$ values. The variation range of $\delta^{18}O$ for the benthic foraminiferal tests ($\sim 2.5‰$) is only slightly lower than for the planktonics ($\sim 3‰$), indicating no significant difference in the degree of diagenetically induced changes.

It can be concluded that equal degrees of alteration would reduce differences in both $\delta^{18}O$ ($\Delta\delta^{18}O$) and $\delta^{13}C$ values ($\Delta\delta^{13}C$) between pairs of planktonic and benthic species, whereas stronger diagenesis of planktonic species compared to the benthic species would reduce $\Delta\delta^{13}C$ and slightly increase $\Delta\delta^{18}O$ (see the insert in Fig. 3). $\delta^{18}O$ values, therefore, cannot be used for absolute temperature calculations, though estimates of temperature differences and variations in surface-to-deep gradients should be valid.

3.2. *Diagenetic effects on Sr/Ca ratios*

Sr/Ca ratios of foraminiferal tests may also be affected by diagenetic alteration. Strontium uptake by foraminifera and incorporation in their tests is known to be higher than Sr concentrations of abiotic calcite (Elderfield et al., 1996). During diagenetic recrystallization, Sr is released from the foraminiferal tests (Richter and Liang, 1993).

Without transport, the Sr^{2+} concentration in the solution rapidly builds up to a point that further reaction could not lower the Sr/Ca of the solid (Baker et al., 1982). Thus, where only minor amounts of Ca are added to or minor amounts of Sr are removed from the system, diagenetic effects will not produce significant changes in the Sr/Ca ratios.

If temperature is the major control, foraminiferal $\delta^{18}O$ and foraminiferal Sr/Ca ratios will be correlated negatively. A strong shift in $\delta^{18}O$ and loss of Sr by the same diagenetic process will produce a positive correlation. However, a moderate diagenetically induced shift in both or in $\delta^{18}O$ alone will shift, weaken, or even destroy an existing negative correlation between $\delta^{18}O$ and Sr/Ca. Differential diagenesis (i.e. different degrees of alteration of benthic and planktonic forms within one sample) results in an overestimation of temperature gradients from $\delta^{18}O$ and an underestimation from Sr/Ca ratios. Thus, the temperature gradients estimated from $\delta^{18}O$ and those estimated from Sr/Ca ratios will diverge. Non-differential diagenesis will reduce temperature gradients from $\delta^{18}O$, but temperature gradients obtained from Sr/Ca ratios remain nearly unchanged. At Elles, $\delta^{18}O$ versus Sr/Ca shows 'remainders' of a negative correlation and similar variation ranges of the $\delta^{18}O$ and Sr/Ca values for both benthic and planktonic foraminiferal tests. This indicates that pairs of benthic and planktonic foraminiferal tests were not seriously affected by differential diagenetic alteration (Fig. 4).

4. Results

4.1. Stable isotopes

$\delta^{13}C$ isotopes: Planktonic $\delta^{13}C$ values at Elles show a progressive decrease through the upper Maastrichtian beginning in the lower part of zone CF2 and continuing into CF1, whereas benthic $\delta^{13}C$ values show a corresponding increase, thus reducing the surface-to-deep gradient. Are these long-term trends primary, or do they reflect an increasing diagenetic overprint from the bottom to the top of the section? Since the difference in $\delta^{18}O$ for planktonic and benthic foraminifera is nearly constant across the entire profile, an increasing diagenetic overprint up-section and serious effects of differential diagenesis seem improbable. The coupled but opposite changes in the isotopic records of the planktonic and benthic species suggest a continuous decrease in surface bioproductivity over the last 400 kyr (zones CF1 and CF2) of the Maastrichtian (Fig. 5). This is also indicated by the surface-to-deep $\delta^{13}C$ gradient, which shows a gradual decrease in zones CF2 and CF1 (Fig. 6).

The decreasing trend in bioproductivity is interrupted by several shorter excursions of higher amplitude in $\delta^{13}C$ values and increased $\Delta^{13}C$ gradients. The first conspicuous deviation in benthic values (0.7‰ negative shift) and increased gradient occur between 21.5 and 23.5 m across the CF2/CF3 boundary (Figs. 5 and 6). The sudden drop in $\delta^{13}C$ values is likely related to terrestrial organic matter influx, rather than bioproductivity, as a result of erosion and a lower sea level, as also observed in other Tunisian sections (Li et al., 2000). The second deviation is a positive excursion in planktonic foraminifera and increased $\Delta^{13}C$ gradient between 2 and 4 m below the K/T boundary, followed by a strongly reduced $\Delta^{13}C$ gradient in the interval just below the K/T boundary. In the shallow shelf environment of the upper Maastrichtian in Tunisia these carbon isotope variations may be related to a combination of changes in bioproductivity, sea level, or secular variations in seawater carbon isotopes.

Comparison of the deep-sea record with that of the Tunisian sections suggests the presence of regional signals. During late Campanian the deep-sea $\delta^{13}C$ record shows relatively low values between 0.5‰ and 1.0‰, as also observed at Elles, and minimum values at the Campanian/Maastrichtian transition (not observed at Elles, though present at El Kef) coincident with maximum global cooling (Barrera, 1994, Barrera et al., 1997; Li and Keller, 1998a,b). However, deep-sea signals and Tunisian continental shelf signals diverged during the Maastrichtian. In the deep sea, $\delta^{13}C$ values increased by 1.5–2‰ in bottom and surface waters in the early Maastrichtian and remained relatively high through the upper Maas-

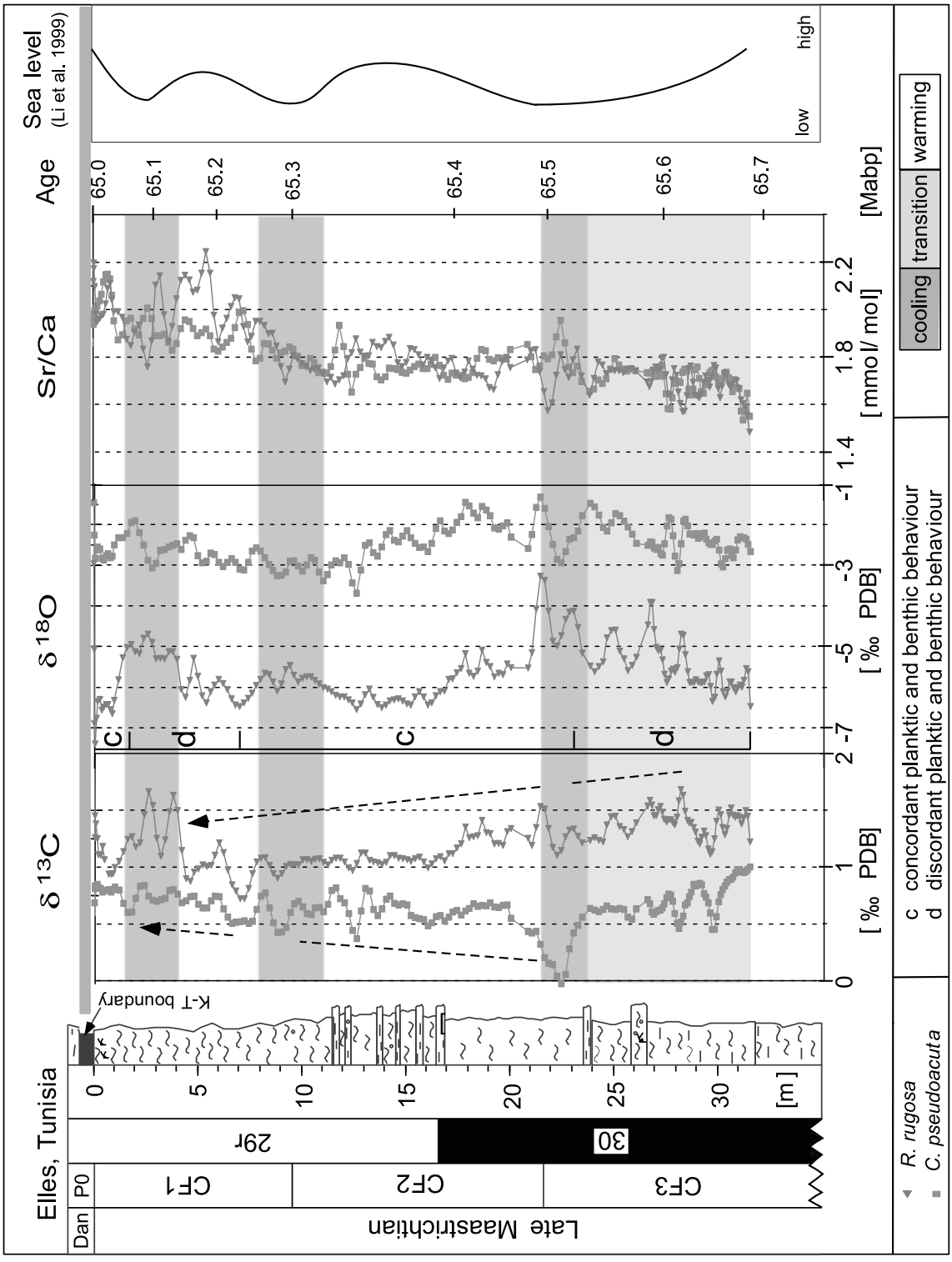

Fig. 5. Late Maastrichtian litholog, $\delta^{18}O$, $\delta^{13}C$, and Sr/Ca profiles of the Elles section for benthic (*Cibicidoides pseudoacuta*) and planktonic (*Rugoglobigerina rugosa*) foraminifera (five-point smoothed data). Dashed arrows indicate the general trend in $\delta^{13}C$ (p = planktonic; b = benthic). The cross-over of Sr/Ca ratios of benthic and planktonic foraminifera is caused by a general inter-species shift of Sr/Ca levels due to differing vital effects of benthic and planktonic foraminifera. Sea level curve after Li et al. (1999). Magnetostratigraphy after Harland et al. (1990).

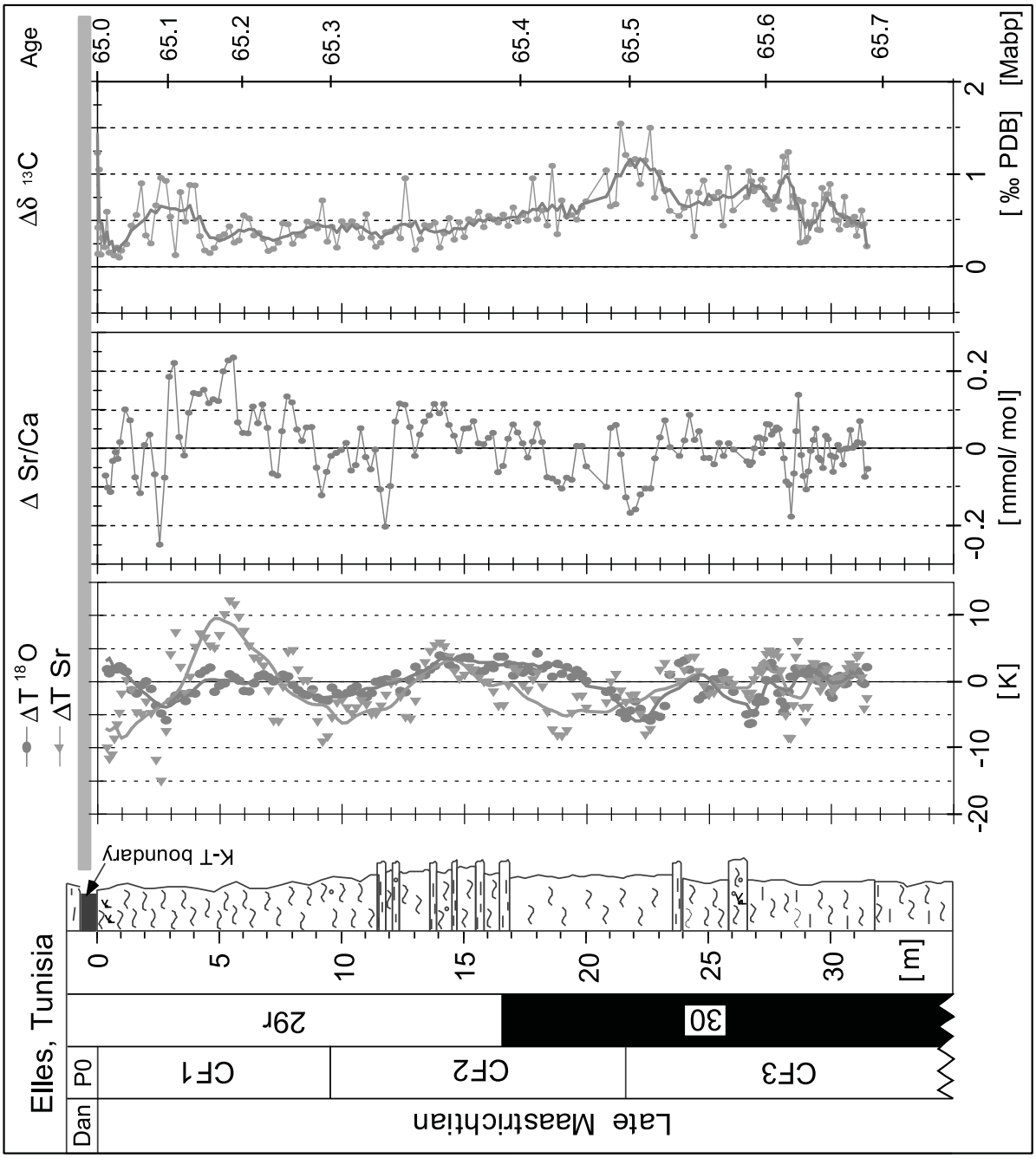
Elles, Tunisia
Late Maastrichtian
Dan
P0
CF1
CF2
CF3
29r
30
K-T boundary
[m]
0
5
10
15
20
25
30
ΔT 18O
ΔT Sr
[K]
10
0
-10
-20
Δ Sr/Ca
[mmol/ mol]
0.2
0
-0.2
Δδ 13C
[‰ PDB]
2
1
0
Age
[Mabp]
65.0
65.1
65.2
65.3
65.4
65.5
65.6
65.7

trichtian (Li et al., 2000). But in Tunisian sections Maastrichtian $\delta^{13}C$ values in surface and deep waters are variable and generally 2–3‰ lower relative to the open ocean (D'Hondt and Lindinger, 1994; Barrera, 1994). Similarly low $\delta^{13}C$ values have been observed in the upper Maastrichtian of Egypt (Keller et al., 2002). This suggests a primarily regional record and reflects a relatively constant terrestrial organic influx of lighter carbon.

$\delta^{18}O$ isotopes: $\delta^{18}O$ values of planktonic and benthic foraminifera display roughly similar trends in low-frequency cycles with varying gradients, but exhibit convergent and divergent episodes in the high-frequency range (Fig. 5). The first convergent episode and minimum surface-to-deep gradient coincide with the benthic $\delta^{13}C$ excursions between 21.5 and 3.5 m and zone CF2/CF3 transition. Benthic and planktonic $\delta^{18}O$ covary and change towards more positive values in this interval, though with a significantly more positive shift in planktonic values. This suggests climatic cooling of both surface and bottom waters in this relatively shallow continental shelf environment. Generally lighter $\delta^{18}O$ values in zone CF2 suggest a period of warming that culminates between 11 and 16 m. A second minimum in the $\Delta^{18}O$ gradient associated with more positive planktonic $\delta^{18}O$ values, indicates cooling between 8 and 11 m at the CF1/CF2 zone boundary. Between 4 and 8 m generally more negative planktonic $\delta^{18}O$ values suggest warming. This interval is followed by strongly oscillating and generally more positive values between 2 and 4 m below the K/T boundary, which suggests unstable climatic and environmental conditions. In the last 2 m below the K/T boundary, benthic and planktonic values covary, followed by an abrupt increase at the K/T boundary (see Stüben et al., 2002, for details of the K/T boundary event).

4.2. Sr/Ca results

The incorporation of Sr into foraminiferal calcite is controlled by the Sr/Ca ratio of seawater, temperature, salinity, pH, pressure, and vital effects (Lea et al., 1999; Rathburn and De Deckker, 1997; Rosenthal et al., 1997). Sea level fluctuations affect Sr flux into the oceans. At times of subsiding sea levels, Sr-rich aragonite from continental shelfs exposed to weathering alters to calcite; because calcite can incorporate less Sr than aragonite, the released Sr is relatively rapidly transported into the oceans (90% of Sr in shelf carbonate within less than 100 000 years; Stoll and Schrag, 1996, 1998). Therefore, sea level fluctuations are characterized by variations in the Sr content of sediment layers and the foraminifera incorporate Sr into their shells in equilibrium with seawater (e.g. Graham et al., 1982; Stoll and Schrag, 1996, 2001). The sea level dependency of the Sr/Ca ratio can be overprinted by the effect of changing temperature, salinity, pH, (Lea et al., 1999; Malone and Baker, 1999) and pressure (Rosenthal et al., 1997; ~100 μmol/mol per 1000 m), as well as by non-equilibrium vital effects. Laboratory experiments revealed that the Sr distribution coefficient between calcite and solution increases with temperature (Malone and Baker, 1999). From live cultures Lea et al. (1999) obtained positive slopes for the dependencies of Sr uptake in foraminiferal calcite with temperature (11–18 μmol/mol per °C), salinity (10 μmol/mol per psu) and pH (69–148 μmol/mol per unit), whereas increasing pressure decreased the Sr uptake by 100 μmol/mol per 1000 m (Rosenthal et al., 1997). The Elles section was deposited at middle to outer neritic depths at ~100 m (Li et al., 1999; Abramovich et al., 2002). Due to low water depth during sediment deposition the pressure dependency can be neglected, but a decreasing sea level may have sig-

Fig. 6. Comparison of temperature differences calculated from $\Delta^{18}O$ and Sr/Ca (ΔSr/Ca) between planktonic and benthic foraminifera. ΔT_{18O} is calculated after Erez and Luz (1992), based on the differences of $\delta^{18}O$. ΔT_{Sr} is calculated from ΔSr/Ca using calibration data from culture experiments (Lea et al., 1999). Dots are raw data, lines are five-point smoothed data. Magnetostratigraphy after Harland et al. (1990).

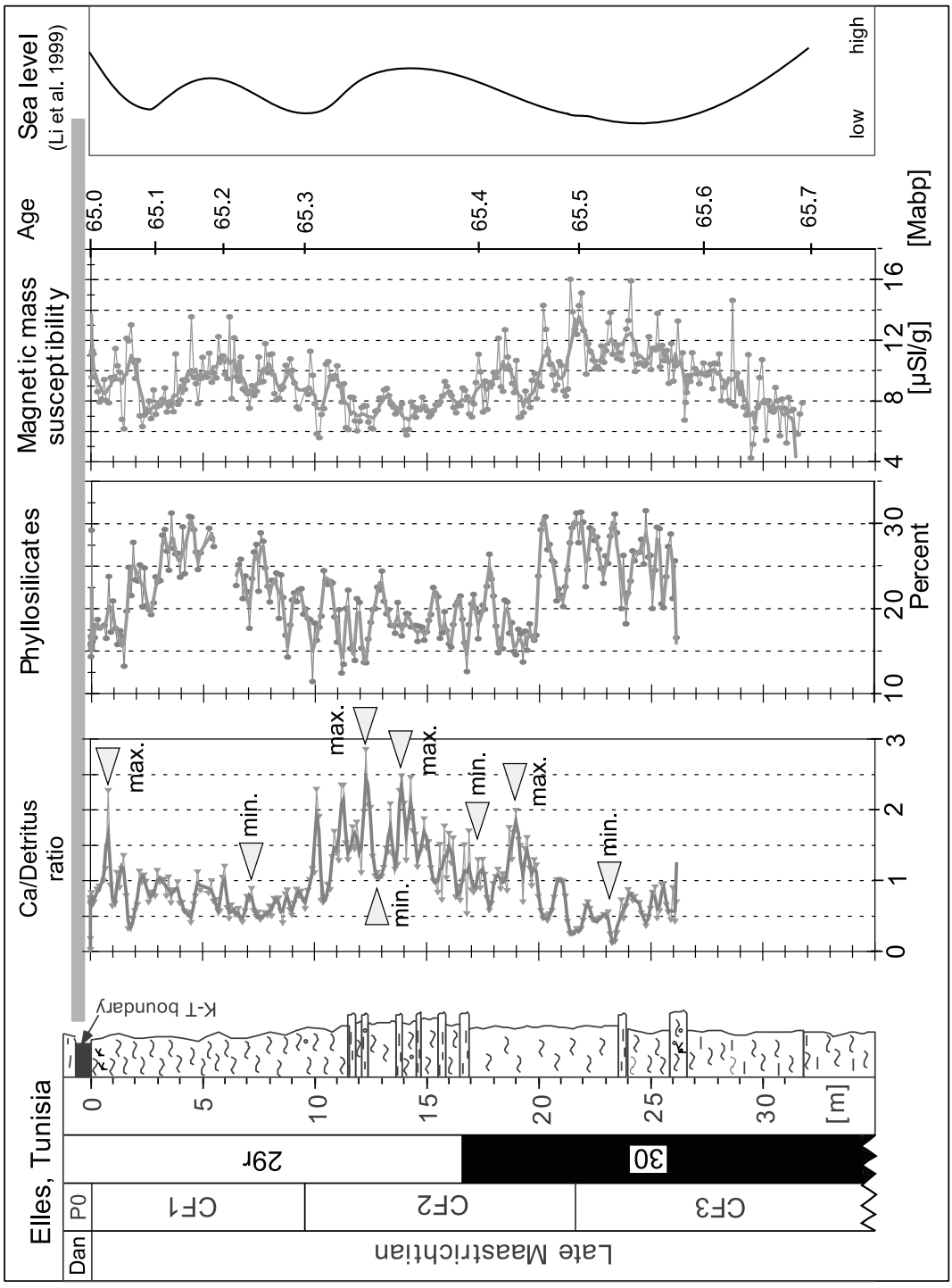

Fig. 7. Late Maastrichtian lithologic, mineralogical composition (phyllosilicates), and calcite/detritus ratio (detritus = quartz+phyllosilicates; magnetic susceptibility raw and five-point smoothed data) of the Elles section in comparison with the sea level curve of Li et al. (1999). Magnetostratigraphy after Harland et al. (1990).

nificantly increased riverine Sr flux into the ocean. For this reason, one might argue for a more rapid response in seawater Sr/Ca ratios in shallow water depositional environments such as Elles than in the deep sea, even though the long residence time of Sr in the water column delays the response to increasing sea levels.

At Elles the Sr/Ca ratios of benthic and planktonic foraminifera generally covary between ratios of 1.6 and 1.8 mmol/mol near the base of the section and between 1.7 and 1.9 mmol/mol through the upper CF3 to CF2 intervals (Fig. 5). In CF1 benthic Sr/Ca values gradually increase between 1.8 and 2.0 mmol/mol with planktonic values significantly higher (up to 2.2 mmol/mol) and strongly fluctuating between 3 and 5 m below the K/T boundary. In the 2 m below the K/T boundary Sr/Ca values of both planktonic and benthic foraminifera reach peak values and then decline near the boundary. Across the entire section Sr/Ca ratios of benthic and planktonic foraminifera increase to the top. If this general trend is mainly temperature controlled, then $\delta^{18}O$ values should display a steady decrease from bottom to top, which is not the case. This indicates that at Elles temperature is not the major control for the Sr/Ca ratios in benthic and planktonic foraminifera.

The increasing Sr/Ca trend suggests lower sea levels near the CF3/CF2 boundary, in the middle of CF1 and again near the top of CF1 (Fig. 5). This interpretation seems to be supported by the high quartz content at the CF3/CF2 transition and a short hiatus or condensed interval, and the high quartz content between 1 and 2 m below the K/T boundary (Fig. 7). But the correlation is not precise and the low detrital influx in CF1 corresponds to the low quartz influx. The relatively poor correlation may be due to the lag-time in the release of Sr to seawater (depending on the sedimentation rate, the lag-time may correspond to 0.2–0.8 m at 10 000 years). Alternatively, the high Sr/Ca values in CF1 may be due to increased chemical weathering, rather than the sea level fall, as suggested by warmer temperatures (Fig. 5) and clay mineralogy that reflects increasingly humid conditions at Elles (Adatte et al., 2002).

Although Sr is presumed to be homogeneous in its distribution in the water column (e.g. de Villiers, 1999), the gradient of the Sr/Ca ratios (ΔSr/Ca) between benthic and planktonic foraminifera varies with depth because of the dependency of the distribution coefficient between seawater and foraminiferal calcite on sea level, salinity, pH, and temperature changes. Consequently, the surface-to-deep gradient of the Sr/Ca ratio will mainly be controlled by the surface-to-deep temperature and/or salinity gradient.

The low but nevertheless significant cross-correlation coefficient ($r = 0.254$, $n = 230$, $P < 0.1\%$) of the surface-to-deep Sr/Ca ratio (ΔSr/Ca) and the $\Delta^{18}O$ surface-to-deep temperature gradient (ΔT, Fig. 6) suggests that the surface-to-deep Sr/Ca ratio is mainly controlled by variations in the temperature difference of surface and bottom waters. Low surface-to-deep Sr/Ca gradients correspond to cool intervals and high gradients to warm climatic intervals. These fluctuations in the Sr/Ca ratios of benthic and planktonic foraminifera may reflect variations between surface water and sediment surface temperatures. Effects of pressure dependency (Rosenthal et al., 1997) related to short-term sea level fluctuations are of minor importance in this shallow water section. Additional variability in the Sr/Ca ratios may be introduced by vital effects (resulting in different Sr contents in planktonic and benthic foraminifera), or by varying local gradients of the Sr concentration in the water column as a consequence of variations in the riverine flux (Stoll et al., 1999).

4.3. Paleotemperature trends

Although diagenetic alteration of foraminiferal tests at Elles shifts the original temperature signals to warmer values, relative changes in planktonic and benthic foraminifera and long-term trends are preserved (e.g. Schrag et al., 1992, 1995; Sakai and Kano, 2001; Pearson et al., 2001). As a result, calculated temperatures, particularly of planktonic species, tend to be significantly higher than the original temperature values. Nevertheless, temperature calculations of somewhat recrystallized planktonic and benthic

foraminiferal tests are useful to evaluate surface-to-deep temperature gradients and watermass stratification. For this purpose, temperature and ΔT values were calculated for both planktonic and benthic species based on Erez and Luz (1992) (Fig. 6). A Sr/Ca_{Foram} thermometer based on the foraminiferal data of Lea et al. (1999) (ΔT_{Sr}) was applied to the variations in the surface-to-deep Sr/Ca gradient for comparison. Differences in salinity of bottom and surface waters are likely due to density differences, with higher salinities expected in bottom waters. Reduced salinity of the surface waters by dilution with fresh water would increase the apparent temperature difference obtained from the $\delta^{18}O$ thermometer, but reduce the temperature difference from the Sr/Ca_{Foram} thermometer. The similar temperature trends and range of variations indicate that the effects of diagenesis and salinity variations of the surface waters on long-term temperature trends are relatively minor.

As would be expected, planktonic foraminifera show greater variations than benthic species because surface waters are more sensitive to temperature fluctuations than bottom waters. Both long-term and short-term trends are apparent. Long-term trends in the lower and upper parts of the Elles section (zones CF3 and CF1 intervals) show relatively close benthic and planktonic values, whereas in zone CF2 they diverge. The same trend is observed in the ΔT_{Sr} and ΔT $\delta^{18}O$ values (Fig. 6). This can be explained by changes in sea level, climate, and mixing of the water column, with all of them influencing the observed temperature trends.

A lower sea level prevailed during deposition of the CF3 interval with a sea level lowstand at the CF2/CF3 boundary (Li and Keller, 1998c; Li et al., 2000; Abramovich et al., 2002). The divergent benthic and planktonic values in zone CF2 correspond to a rising sea level and global climate warming (Stott and Kennett, 1990; Barrera, 1994; Li and Keller, 1998b) and suggest increased watermass stratification. The global warming continued into CF1, accompanied by warmer bottom water temperatures, and was followed by cooling in the uppermost Maastrichtian. At Elles, the climate warming of CF1 appears to be reflected by increased mixing of the water column and somewhat warmer bottom water temperatures. There are also three short-term episodes of strongly convergent $\delta^{18}O$ values that reflect cooling of surface waters and strong mixing of the water column, possibly accompanied by lower sea levels. These episodes occurred at the CF3/CF2 and CF2/CF1 transitions and in the upper part of CF1 (Fig. 6).

4.4. Mineralogy

Relative changes in bulk rock compositions indicate variations in sediment sources and reflect the variable intensity of weathering and erosion under arid and humid climates (Chamley, 1989; Weaver, 1989), as well as the variable influx of terrigenous sediments into the oceans during high and low sea levels. High detrital influx (phyllosilicates and quartz) is generally associated with increased erosion and transport during lower sea levels and seasonally cool climate. In contrast, high carbonate deposition is generally associated with humid warm climates and transgressive seas. At Elles, periods of increased phyllosilicates (Fig. 7) and quartz contents correspond to lower sea levels and increased erosion near the CF3/CF2 boundary and near the top of the section below the K/T boundary. In zone CF2, the decreased detrital influx (lower quartz and phyllosilicates) suggests a rising sea level, whereas a decreasing sea level is suggested in CF1 by decreased quartz, but high phyllosilicate content. The sea level changes inferred from mineralogical proxies are supported by sea level changes from biostratigraphic data (Li et al., 1999, 2000), which reveal sea level lowstands at ~21 m (65.5 Ma) and a rapidly decreasing sea level in the uppermost 3 m (100 kyr) of the Maastrichtian. The time control is calculated from the sedimentation rates derived from variations of the cyclicity of the magnetic mass susceptibility data discussed below.

The general trend of increasing calcite/detritus ratios between ~21 m (65.5 Ma) and 3 m (65.1 Ma) is overlain by high- and low-frequency sinoidal fluctuations, which show minima suggesting lower sea levels at ~23 m (~65.53 Ma), ~15–18 m (65.40–65.44 Ma), 13 m (65.38 Ma), and ~8 m (65.27 Ma). Maxima in Ca/detritus ratios

indicate higher sea levels at ~19 m (65.46 Ma), ~14 m (~65.39 Ma), 12 m (65.36 Ma) and 1 m (~65.03 Ma, Fig. 6). These local sea level variations derived from the Ca/detritus ratio at Elles generally coincide with the sea level curve of Li et al. (1999) from mid-Atlantic DSDP Site 525A.

4.5. Magnetic mass susceptibility

Magnetic susceptibility of sediments is related to the mineralogical composition of the sediments and depends on grain size and concentration of magnetic minerals. Only Fe-bearing rock-forming minerals show positive susceptibility, with ferrimagnetic minerals, like magnetite, orders of magnitudes higher than the susceptibility of all other rock-forming minerals. Thus, even in low concentrations these minerals dominate the bulk susceptibility of sediments (Dekkers, 1997). Sea level changes alter the detrital input, resulting in possible shifts in mineral sources and types. In the supposedly ice-free world of the late Cretaceous, sea level changes are unlikely to be driven by Milankovich forcing although weathering conditions strongly depend on climate, which is influenced by variations in insolation. Changing weathering conditions mainly affect riverine input and eolian influx, which effectively act in the Milankovich frequency range (Tauxe, 1993).

At Elles, magnetic mass susceptibility varies from 4 to 16 μSI/g and generally mimics the trend of phyllosilicates with a reasonable correlation between intervals of high phyllosilicates and high magnetic susceptibility ($r = 0.48$, $n = 291$, $P < 0.00$; Fig. 7). The long-term quartz trend does not correlate with either phyllosilicates or magnetic susceptibility in zone CF1, possibly due to changes in climate to more humid seasonal cool conditions and hence decreased quartz transport (Adatte et al., 2002). Moreover, short-term cycles are evident with a good correlation between increased phyllosilicate input and high magnetic susceptibility.

The magnetic susceptibility record at Elles thus exhibits both a long-term trend and short-term variations in the amount and composition of terrigenous sediment flux relative to biogenic carbonate production, and these are governed by climate and local sea level changes. Magnetic susceptibility is tracking changes in weathering intensity on adjacent continents and, unlike sea level changes in an ice-free world, they likely vary with Milankovich-driven climate variations.

4.6. Time series analysis

To determine periodicities in the sediment column at Elles, time series analysis was performed on magnetic mass susceptibility data and the Sr/Ca and C and O isotope values of benthic (*Cibicidoides pseudoacuta*) and planktonic (*Rugoglobigerina rugosa*) foraminifera. Before applying time series analysis, variations in sedimentation rates were evaluated based on susceptibility and biostratigraphic data. Based on planktonic foraminiferal biostratigraphic data sediment accumulation rates for the combined CF1–CF2 interval averages of 4.88 cm/kyr, or 3.2 cm/kyr for CF1 and 8 cm/kyr for CF2 were obtained.

In the susceptibility data two main short cycles are apparent with high-frequency variations superimposed at about 0.8–1.0 m and 1.6 m intervals (Fig. 7). This suggests the presence of 20 kyr and 40 kyr cycles based on biostratigraphic age correlations and an average sediment accumulation rate of 4.88 cm for the CF1–CF2 interval, which spans the 450 kyr of chron 29R below the K/T boundary (Li and Keller, 1998a,b). The dominating very low frequent sinoidal periodicity of the susceptibility data is assumed to represent the ~400 kyr Milankovich cycle. The wavelength of this periodicity increases with depth. The clearly visible elongated periodicity in the lower half of the profile reflects increased sedimentation rates in CF2/CF3 as compared to CF1.

To account for the effects of varying sedimentation rates, a sinus function was fitted to the long periodicity, and the sedimentation rate was stepwise adjusted in order to get the best possible fit for the long periodicity. After this stepwise adjustment, estimated sedimentation rates average 3.2 cm/kyr for the interval between 0 and 6.4 m (~65–65.2 Ma), 2.5 cm/kyr for the interval between 6.6 and 9.8 m (~65.2–65.3 Ma), 8 cm/kyr between 9.8 and 17.6 m (~65. 3–65.4 Ma), and 5 cm/kyr for the older succession (17.8–31.45 m). The average adjusted sedimentation rate is 5.04

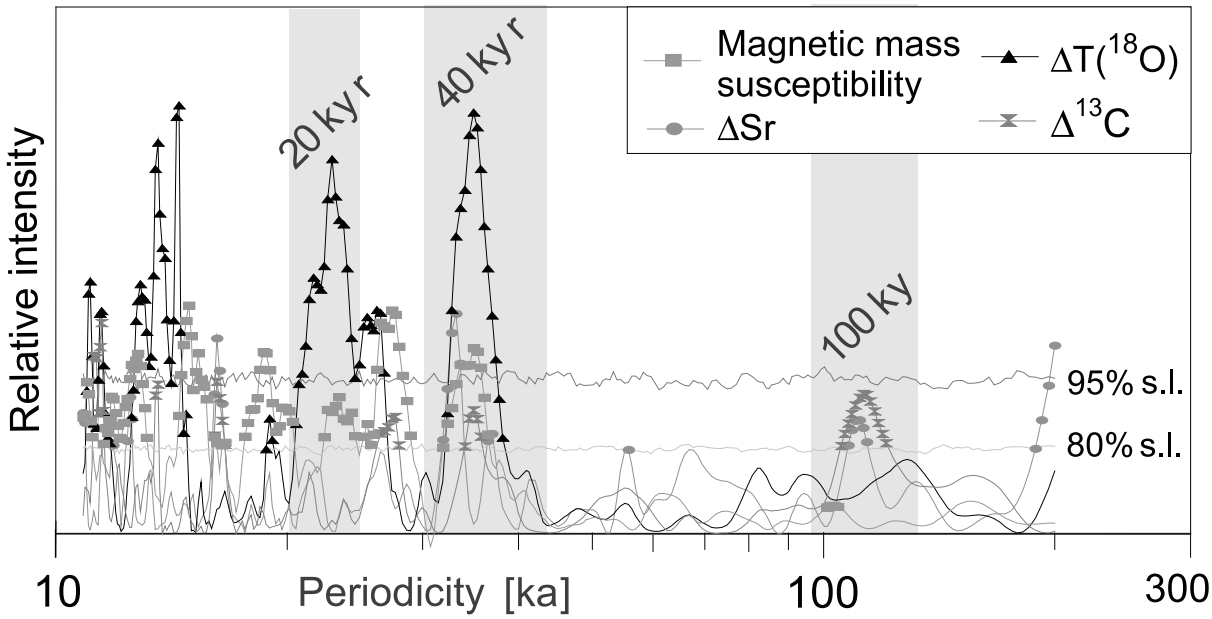

Fig. 8. Red noise normalized energy spectrum of the periodicities from time series analysis of magnetic mass susceptibility, $\Delta\delta^{18}O$, and $\Delta Sr/Ca$ for the Elles Maastrichtian section showing 20, 40, and 100 kyr Milankovitch cycles. The lines 95% s.l. and 80% s.l. mark the Monte Carlo simulations of the 95% and 80% significance levels. The time series analysis is based on sedimentation rates of 3.2 cm/kyr for CF 1, 2.5 cm/kyr for CF2, and 5–8 cm/kyr for CF2 to CF3.

cm/kyr for CF1 and CF2, which is close to the average sedimentation rate of 4.88 cm/kyr estimated from biostratigraphy. Similar results were obtained by adjusting the sedimentation rates based on fitting the 20 kyr cycle to the susceptibility record (Hambach and Adatte, 2000).

Based on these stepwise adjusted sedimentation rates, time series analysis was carried out using the REDFIT program (Schulz and Mudelsee, 2002), in order to isolate the shorter Milankovich cycles (20, 40 and 100 kyr). REDFIT is based on the SPECTRUM algorithm (Schulz and Stattegger, 1997), which allows the analysis of unevenly spaced time series. REDFIT estimates the red noise spectra from unevenly spaced time series by fitting a first order autoregressive, AR1, function. To reduce the effects of white noise the raw data were smoothed by a five-point moving average, using weights derived from a parabolic smoothing function (Savitzky and Golay, 1964).

The resulting periodograms for $\delta^{18}O$, $\delta^{13}C$, and Sr/Ca ratios for benthic and planktonic foraminifera as well as for the magnetic susceptibility display clear low and short periodicities of 20 ± 3, 40 ± 5 and 100 ± 15 kyr, which correspond to Milankovich cycles. However, the peaks are below the 80% false alarm level for red noise, except for susceptibility data. For the surface-to-deep gradients, $\Delta^{18}O$ (ΔT), $\Delta^{13}C$, and ($\Delta Sr/Ca$), these cyclicities are more pronounced and the 20 kyr precision cycle, 40 kyr obliquity cycle, and eccentricity cycle of $\sim$100 kyr can be identified at the 80% and for ΔT at the 95% significance level (Fig. 8). A 60 kyr resonance (possibly the half of the 127 kyr eccentricity cycle) is present in the periodograms of $\delta^{18}O$, $\delta^{13}C$, and Sr/Ca ratios for benthic and planktonic foraminifera, but is not traceable in the surface-to-deep gradients.

5. Discussion

5.1. Climate and productivity: the last 700 kyr of the Maastrichtian

During the last 700 kyr of the Maastrichtian the eastern Tethys (Tunisia) experienced major variations in climate and productivity that reflect

global paleoceanographic changes. Based on a high-resolution database that includes various paleoceanographic proxies, including $\delta^{13}C$, $\delta^{18}O$, Sr/Ca, mineralogical and magnetic susceptibility data of the Elles section in Tunisia, the environmental history can be reconstructed.

Between 65.7 and 65.5 Ma (CF3) relatively high but gradually decreasing $\delta^{18}O$ values, a fluctuating and decreasing surface-to-deep temperature gradient, and an increasing $\delta^{13}C$ gradient indicate climate cooling and relatively high productivity. A major positive excursion in $\delta^{18}O$ between 65.50 and 65.55 Ma (CF3/CF2 boundary, 21.5–23.5 m) marks maximum upper Maastrichtian cooling (Figs. 5 and 6), whereas the fluctuating $\delta^{18}O$ values, and very low surface-to-deep Sr/Ca ratios and temperature gradients indicate strong mixing of the water column during cooling (Figs. 5 and 6). The major drop in benthic $\delta^{13}C$ values, but only minor decrease in surface waters, probably reflects changes in carbon isotopes of the oceanic total dissolved carbon, and increased carbon flux due to erosion and weathering related to the climatic cooling and accompanying sea level fall. This stratigraphic interval corresponds to a global cooling maximum in the upper Maastrichtian (Barrera, 1994; Barrera et al., 1997; Li and Keller, 1998a,b), associated with a sea level fall and widespread hiatus (Haq et al., 1987; Keller and Stinnesbeck, 1996; Li et al., 1999, 2000). A short hiatus or condensed interval may be present at this interval at Elles as suggested by abrupt faunal, isotopic, and mineralogical changes (Figs. 5 and 7; Adatte et al., 2002; Abramovich and Keller, 2002).

After the cooling maximum, surface and bottom water temperatures rapidly increased, reaching the first of two warm events in CF2 (12–16 m, 65.33–65.38 Ma), whereas the $\delta^{13}C$ gradient gradually decreased due to lower surface $\delta^{13}C$ values. This warm event marks the onset of a global short-term warming which is best documented at DSDP Site 525 (Walvis Ridge, mid-latitude South Atlantic), where temperatures are estimated to have increased by 3–4°C in both surface and intermediate waters (Li and Keller, 1998b), but the same warm event has also been recognized in numerous other deep-sea sections from high to low latitudes (Shackleton et al., 1984; Stott and Kennett, 1990; Barrera et al., 1997; Olsson et al., 2001). A warming-up period indicates oceanic turnover and probably decreasing thermohaline circulation during a sea level rise and consequently decreasing productivity. The likely cause for this short-term global warming is increased greenhouse gases probably from major Deccan Trap volcanism estimated between 65.2 and 65.4 Ma (Courtillot et al., 1988, 1996; Baski, 1994; Hoffmann et al., 2000).

Surface waters cooled markedly across the CF2–CF1 transition (11–8 m, 65.33–65.26 Ma) and productivity continued to decrease as indicated by decreasing surface $\delta^{13}C$, and $\Delta^{13}C$ gradients. Another short-term warming in CF1 (8–4 m, 65.26–65.12 Ma) and strongly diverging Sr/Ca suggest an increased surface-to-deep temperature gradient during the upper Maastrichtian. At this time, primary productivity reached minimum values for the upper Maastrichtian, as indicated by major decreases in surface and bottom water $\delta^{13}C$ and a decreasing surface-to-deep gradient (Figs. 5 and 6).

Major climate cooling occurred in surface waters during the upper part of CF1 (2–4 m, 65.12–65.04 Ma) and was accompanied by high but variable primary productivity fluxes and strong mixing evident in Sr/Ca ratios. This short-term cooling phase was also observed in the South Atlantic Site 525A (Li and Keller, 1998a) and reflects a change in watermasses. The increase in surface productivity probably triggered a change in the isotope composition of the total dissolved inorganic carbon reservoir, which may have been enhanced by increased carbon burial and decreased carbon flux from weathering due to a sea level transgression.

The last 40 kyr below the K/T boundary are marked by very unstable paleo-oceanographic conditions, rapid warming, and strong mixing of surface and bottom waters. The surface-to-deep temperature gradient decreased to almost zero, which corresponds to a decrease in the Sr/Ca ratio of planktonic foraminifera. Surface productivity decreased dramatically while the productivity of benthic foraminifera increased slightly. Similar observations were made based on carbon isotope

studies from various localities (South Atlantic, El Kef, Stevns Klint, Nye Kløv) but were interpreted as a consequence of increasing benthic values, rather than decrease in surface productivity (Keller and Lindinger, 1989; Schmitz et al., 1992; Keller et al., 1993; Li and Keller, 1998a). This suggests that the benthic carbon isotope increase during the last 100 kyr of the Maastrichtian primarily reflects changes in the rate and source of deep water productivity, rather than reduced organic carbon oxidation as a result of lower surface productivity (Zachos and Arthur, 1986).

6. Summary and conclusions

High-resolution $\delta^{13}C$, $\delta^{18}O$, Sr/Ca, mineralogical and magnetic susceptibility measurements of hemipelagic sediments spanning the last 700 kyr at Elles, Tunisia, indicate major changes in climate, productivity and sea level. Although diagenetically overprinted, the general trends are preserved in stable isotopes, Sr/Ca, the surface-to-deep gradient, and mineralogical and susceptibility records. The following conclusions can be reached:

(1) Correlations of ΔT (derived from $\Delta^{18}O$ and ΔSr), primary productivity ($\Delta^{13}C$), and magnetic susceptibility with Milankovich cycles indicate that climate, weathering, and nutrient conditions in the Kasserine Island area are mainly driven by variations in insolation, whereas sea level changes during the presumably ice-free Cretaceous world are assumed to be tectonically driven.

(2) Climate changes observed in $\delta^{18}O$ of planktonic foraminifera are more pronounced in the surface-to-deep gradients of $\Delta^{18}O$ and ΔSr.

(3) Cooling between 65.7 and 65.5 Ma coincides with increased $\delta^{13}C$ values, very low Sr/Ca ratios, and a major sea level fall that indicates strong mixing of waters and increased carbon flux due to erosion.

(4) Rapid warming occurred between 65.38 and 65.33 Ma and was accompanied by a decrease in surface productivity that continued through the subsequent rapid cooling of surface waters between 65.33 and 65.26 Ma (CF2–CF1 transition).

(5) The long-term trend in decreasing primary productivity parallels a sea level rise between 65.4 and 65.2 Ma (zones CF2 and CF1) and is probably due to decreased thermohaline circulation associated with climate warming.

(6) During the last 200 kyr of the Maastrichtian, rapidly increasing Sr/Ca ratios associated with warm and cool temperatures may be related to increased chemical weathering and changes in bioproductivity, rather than a sea level fall, as suggested by clay mineralogy.

The results from the Elles succession demonstrate that it is possible to separate paleoclimatic from diagenetic signals by using a multiproxy approach, assuming that the response to diagenesis is systematically different for each proxy. Correlation of the climate, productivity and sea level trends at Elles with similar trends at DSDP Site 525A in the mid-latitude South Atlantic supports this approach and also indicates that these are global, rather than local trends.

Acknowledgements

This study was funded by the Deutsche Forschungsgemeinschaft (STU 169/20-1, Sti 128/4-1), NSF INT 95-04309 (G.K.), the Swiss National Fund No. 8220-028367, and US-Israel Binational Foundation (BSF) Grant 9800425. Markus Leosson is greatly acknowledged for the measurement of the stable isotope. We thank the reviewer H. Stoll and B. Malmgren for their helpful comments and suggestions for improvement of this manuscript.

References

Abramovich, S., Almogi-Labin, A., Benjamini, C., 1998. Decline of the Maastrichtian pelagic ecosystem based on planktic foraminiferal assemblage changes: Implications for the terminal Cretaceous faunal crisis. Geology 26, 63–66.

Abramovich, S., Keller, G., 2002. High stress late Maastrichtian paleoenvironment: inference from planktic foraminifera in Tunisia. Palaeoceanogr. Palaeoclimatol. Palaeoecol. 178, 145–164.

Abramovich, S., Keller, G., Adatte, T., Stinnesbeck, W., Hottinger, L., Stüben, D., Berner, Z., Ramanivosoa, B., Randriamanantenasoa, A., 2002. Age and Paleoenvironment of the Maastrichtian-Paleocene of the Mahajanga Basin, Ma-

dagascar: a multidisciplinary approach. Mar. Miccropaleontol. 47, 17–70.
Adatte, T., Stinnesbeck, W., Keller, G., 1996. Lithostratigraphic and mineralogic correlation of near K/T boundary clastic sediments in northeastern Mexico; implications for origin and nature of deposition. In: Ryder G., Fastovsky, D., Gastner, S. (Eds.), the Cretaceous-Tertiary Event and other Catastrophes in Earth History. Geol. Soc. Am. Spec. Pap. 307, 211–226.
Adatte, T., Keller, G., Stinnesbeck, W., 2002. Late Cretaceous to early Paleocene climate and sea level fluctuations; the Tunisian record. Palaeogeogr. Palaeoclimatol. Palaeoecol. 178, 165–196.
Baker, P.A., Gieskes, J.M., Elderfield, H., 1982. Diagenesis of carbonates in deep-sea sediments – evidence from Sr/Ca ratios and interstitial dissolved Sr^{2+} data. J. Sediment. Petrol. 52, 71–82.
Barrera, E., 1994. Global environmental changes preceding the Cretaceous-Tertiary boundary: early-late Maastrichtian transition. Geology 22, 877–880.
Barrera, E., Huber, B.T., 1990. Evolution of Antarctic waters during the Maastrichtian: Foraminifera oxygen and carbon isotope ratio, Leg 113. Proc. ODP Sci. Results 113, 813–827.
Barrera, E., Savin, S.M., Thomas, E., Jones, C.E., 1997. Evidence for thermohaline-circulation reversals controlled by sea level change in the latest Cretaceous. Geology 25, 715–718.
Baski, A.K., 1994. Geochronological studies on whole-rock basalts, Deccan Traps, India; evaluation of the timing of volcanism relative to the K-T boundary. Earth Planet. Sci. Lett. 121, 43–56.
Bédard, P., Hillaire-Marcel, C., Pagé, P., 1981. ^{18}O modelling of freshwater inputs in Baffin Bay and Canadian Arctic coastal waters. Nature 293, 287–289.
Burollet, P.F., 1967. General Geology of Tunisia. Pet. Explor. Soc. Libya, 9th Annu. Field Conf., Tripoli, pp. 51–58.
Chamley, H., 1989. Clay Sedimentology. Springer, 623 pp.
Courtillot, V., Feraud, G., Maluski, H., Vandamme, D., Moreau, M.G., Besse, J., 1988. Deccan flood basalts and the Cretaceous/Tertiary boundary. Nature 333, 843–846.
Courtillot, V., Jaeger, J.J., Yang, Z., Feraud, G., Hofmann, C., 1996. The influence of continental flood basalts on mass extinctions; where do we stand? In: Ryder, G., Fastovosky, D., Gartner, S. (Eds.), The Cretaceous-Tertiary Event and Other Catastrophes in Earth History. Geol. Soc. Am. Spec. Pap. 307, 513–525.
Dekkers, M.J., 1997. Environmental magnetism: an introduction. Geol. Mijnbouw 76, 163–182.
de Villiers, S., 1999. Seawater strontium and Sr/Ca variability in the Atlantic and Pacific oceans. Earth Planet. Sci. Lett. 171, 623–634.
D'Hondt, S., Lindinger, M., 1994. A stable isotopic record of the Maastrichtian ocean-climate system: south Atlantic DSDP Site 528. Palaeogeogr. Palaeoclimatol. Palaeoecol. 112, 363–378.
Elderfield, H., Bertram, C.J., Erez, J., 1996. A biomineralization model for the incorporation of trace elements into foraminiferal calcium carbonate. Earth Planet. Sci. Lett. 142, 409–423.
Erez, J., Luz, B., 1992. Temperature control of oxygen-isotope fractionation of cultured planktonic foraminifera. Nature 297, 220–222.
Faure, G. 1986. Principles of Isotope Geology, 2nd edn. Wiley, 589 pp.
Graham, D.W., Bender, M.L., Williams, D.F., Keigwin, L.D., Jr., 1982. Strontium calcium ratios in Cenozoic planktonic foraminifera. Geochim. Cosmochim. Acta 46, 1281–1292.
Hambach, U., Adatte, T., 2000. High-resolution magnetic susceptibility records from the Maastrichtian and Lower Paleocene of NW Tunesia. Sixth Int. Cretaceous Symp., Vienna.
Hambach, U., Rose, Th., Krumsiek, K., 2002. Magnetic susceptibility measurements on reseach cores kirchrode I and II: indication for sea level variations and Milankovitch forced cyclicity in the Albian. Cretac. Res. (submitted).
Haq, B.U., Hardenbol, J., Vail, P.R., 1987. Chronology of fluctuating sea levels since the Triassic. Science 235, 1156–1167.
Harland, W.B., Armstrong, R.L., Cox, A.V., Craig, L.E., Smith, A.G., Smith, D.G., 1990. A geologic time scale, 1989. Cambridge Earth Science Series. Cambridge University Press, Cambridge, 131 pp.
Hoffmann, C., Feraud, G., Courtillot, V., 2000. $^{40}Ar/^{39}Ar$ dating of mineral separates and whole rocks from the Western Ghats lava pile: further constraints on duration and age of Deccan traps. Earth Planet. Sci. Lett. 180, 13–27.
Jenkyns, H.C., Gale, A.S., Corfield, R.M., 1994. Carbon- and oxygen-isotope stratigraphy of the English Chalk and Italian Scaglia and its paleoclimatic significance. Geol. Mag. 131, 1–34.
Keller, G., Lindinger, M., 1989. Stable isotope, TOC and $CaCO_3$ records across the Cretaceous/Tertiary boundary at El Kef, Tunisia. Palaeogeogr. Palaeoclimatol. Palaeoecol. 73, 243–265.
Keller, G., Barrera, E., Schmitz, B., Matsson, E., 1993. Gradual mass extinction, species survivorship, and long term environmental changes across the Creataceous-Tertiary boundary in high latitudes. Geol. Soc. Am. Bull. 105, 979–997.
Keller, G., Stinnesbeck, W., 1996. Sea level changes, clastic deposits and megatsunamis across the Cretaceous-Tertiary boundary. In: MacLeod, N., Keller, G. (Eds.), Cretaceous/Tertiary Boundary Mass Extinction: Biotic and Environmental Changes. W.W. Norton, New York, pp. 415–450.
Keller, G., Adatte, T., Stinnesbeck, W., Luciani, V., Karoui, N., Zaghbib-Turki, D., 2002. Paleobiogeography of the Cretaceous-Tertiary mass extinction in planktic foraminifera. Palaeogeogr. Palaeoclimatol. Palaeoecol. 178, 257–298.
Khim, B.-K., Park, B.K., 2000. Recent change of hydrographic features in the Cheju Strait (southeastern Yellow Sea), Korea: contrast between planktonic and benthic foraminifera isotope composition. Mar. Geol. 169, 411–419.
Kucera, M., Malmgren, B.A., 1998. Terminal Cretaceous warming event in the mid-latitude South Atlantic Ocean; evidence from poleward migration of Contusotruncana con-

tusa (planktonic Foraminifera) morphotypes. Palaeogeogr. Palaeoclimatol. Palaeoecol. 38, 1–15.
Lea, D., Mashiotta, T., Spero, H., 1999. Controls on magnesium and strontium uptake in planktonic foraminifera determined by live culturing. Geochim. Cosmochim. Acta 63, 2369–2379.
Li, L., Keller, G., 1998a. Maastrichtian climate, productivity and faunal turnovers in planktic foraminifera in south Atlantic DSDP Sites 525 A and 21. Mar. Micropaleontol. 33, 5–86.
Li, L., Keller, G., 1998b. Diversification and extinction in Campanian-Maastrichtian planktic Foraminifera of northwestern Tunisia. Eclogae Geol. Helv. 91, 75–102.
Li, L., Keller, G., 1998c. Abrupt deep-sea warming at the end of the Cretaceous. Geology 26, 995–998.
Li, L., Keller, G., 1999. Variability in Late Cretaceous climate and deep waters: evidence from stable isotope. Mar. Geol. 161, 171–190.
Li, L., Keller, G., Stinnesbeck, W., 1999. The Late Campanian and Maastrichtian in northwestern Tunisia: paleoenvironmental inferences from lithology, macrofauna and benthic foraminifera. Cretac. Res. 20, 231–252.
Li, L., Keller, G., Adatte, T., Stinnesbeck, W., 2000. Late Cretaceous sea level changes in Tunisia: a multi-disciplinary approach. J. Geol. Soc. Lond. 157, 447–458.
Malone, M., Baker, P., 1999. Temperature dependence of the strontium distribution coefficient in calcite; an experimental study from 408 degrees to 2008 degrees C and application to natural diagenetic calcites. J. Sediment. Res. 69, 216–223.
Martin, J.M., Letolle, R., 1979. Oxygen 18 in estuaries. Nature 282, 292–294.
McLeod, K.G., Huber, B.T., Pletsch, T., Röhl, U., Kucera, M., 2001. Maastrichtian foraminiferal and paeoceanographic changes on Milankovitch timescales. Paleoceanography 16, 133–154.
Mitchell, S.F., Ball, J.D., Crowley, S.F., Marshall, J.D., Paul, C.R.C., Veltkamp, C.J., Samir, A., 1997. Isotope data from cretaceous chalks and foraminifera: Environmental or diagenetic signals? Geology 25, 691–694.
Olsson, R.K., Wright, J.D., Miller, K.G., 2001. Paleobiogeography of Pseudotextularia elegans during the latest Maastrichtian global warming event. J. Foraminif. Res. 31, 275–282.
O'Neil, J.R., 1987. Preservation of H, C, O isotopic ratios in the low temperature environment. In: Kyser, T.K. (Ed.), Short Course in Stable Isotope Geochemistry of Low Temperature Fluids. Miner. Assoc. Can., pp. 85–128.
Pearson, P.N., Ditchfield, P.W., Singano, J., Harcourt-Brown, K.G., Nicholas, C.J., Olsson, R.K., Shackleton, N.J., Hall, M.A., 2001. Warm tropical sea surface temperatures in the Late Cretaceous and Eocene epochs. Nature 413, 481–487.
Pierre, Ch., 1999. The carbon and oxygen isotope distribution in the Mediterranean water mases. Mar. Geol. 153, 41–55.
Rathburn, A.E., De Deckker, P., 1997. Magnesium and strontium compositions of recent benthic foraminifera from the Coral Sea, Australia and Prydz Bay, Antarctica. Mar. Micropaleontol. 32, 231–248.
Richter, F.M., Liang, Y., 1993. The rate and consequences of Sr diagenesis in deep-sea carbonates. Earth Planet. Sci. Lett. 177, 553–565.
Rohling, E.J., de Rijk, S., 1999. Holocene Climate Optimum and Last Glacial Maximum in the Mediterranean: the marine oxygen isotope record. Mar. Geol. 153, 57–75.
Rosenthal, Y., Boyle, E.D., Slowley, N., 1997. Temperature control on the incorporation of magnesium, strontium, fluorine and cadmium into benthic foraminiferal shells from Little Bahama Bank: Prospects for thermocline paleoceanography. Geochim. Cosmochim. Acta 61, 3633–3643.
Sakai, S., Kano, A., 2001. Original oxygen isotopic composition of planktic foraminifera preserved in diagenetically altered Pleistocene shallow-marine carbonates. Mar. Geol. 172, 197–204.
Savitzky, A., Golay, M.J.E., 1964. Smoothing and differentiation of data by simplified least squares procedures. Anal. Chem. 36, 1627–1639.
Schmidt, G.A., 1999. Forward modelling of carbonate proxy data from planktonic foraminifera using oxygen isotope tracers in a global ocean model. Paleoceanography 14, 482–497.
Schmitz, B., Keller, G., Stenvall, O., 1992. Stable isotope and foraminiferal changes across the Cretaceous/Tertiary boundary at Stevns Klint, Denmark: Arguments for long-term oceanic instability before and after bolide impact. Palaeogeogr. Palaeoclimatol. Palaeoecol. 96, 233–260.
Schrag, D.P., 1999. Effects of diagenesis on the isotopic record of late paleogene tropical sea surface temperatures. Chem. Geol. 161, 215–224.
Schrag, D.P., DePaolo, D.J., Richter, F., 1992. Oxygen isotope exchange in a two-layer model of oceanic crust. Earth Planet. Sci. Lett. 111, 305–317.
Schrag, D.P., DePaolo, D.J., Richter, F.M., 1995. Reconstructing past sea surface temperatures: correcting for diagenesis of bulk marine carbon. Geochim. Cosmochim. Acta 59, 2265–2278.
Schulz, M., Mudelsee, M., 2002. Spectrum: Spectral analysis of unevenly spaced paleoclimatic time series. Comput. Geosci. 23, 929–945.
Schulz, M., Stattegger, K., 1997. REDFIT: estimating rednoise spectra directly from unevenly spaced paleoclimatic time series. Comput. Geosci. 28, 421–426.
Scotese, C.R., Sager, W.W., 1988. Plate tectonic reconstructions of the Cretacious and Cenozoic ocean basins. Tectonophysics 155, 27–48.
Shackleton, N.J., Hall, M.A., Boersma, A., 1984. Oxygen and carbon isotope data from Leg 74 foraminifera. DSDP Init. Rep. 74, 599–612.
Spero, H.J., Bijma, J., Lea, D.W., Bemis, B.E., 1997. Effect of seawater carbonate concentration on foraminiferal carbon and oxygen isotopes. Nature 390, 497–500.
Spicer, R.A., Corfield, R.M., 1992. A review of terrestrial and marine climates in the Cretaceous with implications for modeling the 'Greenhouse'. Earth Geol. Mag. 129, 2, 169–180.
Stinnesbeck, W., Schulte, P., Lindenmaier, F., Adatte, T.,

Affolter, M., Schilli, L., Keller, G., Stueben, D., Berner, Z., Kramar, U., Burns, S.J., Lopez-Oliva, J.G., 2001. Late Maastrichtian age of spherule deposits in northeastern Mexico; implication for Chicxulub scenario. Can. J. Earth Sci. 38, 229–238.

Stoll, H.M., Schrag, D.P., 1996. Evidence for glacial control of rapid sea level changes in the early Cretaceous. Science 272, 1771–1774.

Stoll, H.M., Schrag, D.P., 1998. Effects of Quaternary sea level cycles on strontium in seawater. Geochim. Cosmochim. Acta 62, 1107–1118.

Stoll, H.M., Schrag, D.P., Clemens, S.C., 1999. Are seawater Sr/Ca variations preseved in Quaternary foraminfera? Geochim. Cosmochim. Acta 63, 3535–3547.

Stoll, H.M., Schrag, D.P., 2001. Sr/Ca variations in Cretaceous carbonates: relation to productivity and sea level changes. Palaeoceanogr. Palaeoclimatol. Palaeoecol. 168, 311–336.

Stott, L.D., Kennett, J.P., 1990. The paleoceanographic and paleoclimatic signature of the Cretaceous/Paleogene boundary in the Antarctic: Stable isotopic results from ODP Leg 113. Proc. ODP Sci. Results 113, 829–848.

Stüben, D., Kramar, U., Berner, Z., Stinnesbeck, W., Keller, G., Adatte, Th., 2002. Trace elements and stable isotopes in foraminifera of the Elles II K/T profile: Indications for sea level fluctuations and primary productivity. Palaeogeogr. Palaeoclimatol. Palaeoecol. 178, 321–345.

Tauxe, L., 1993. Sedimentary records of relative paleointensity of the geomagnetic field: theory and practice. Rev. Geophys. 31, 319–354.

Weaver, C.E., 1989. Clays, Muds and Shales. Developments in Sedimentology. Elsevier, 44 pp.

Wolff, T., Grieger, B., Hale, W., Dürkoop, A., Mulitza, S., Pätzold, J., Wefer, G., 1999. On the reconstruction of Paleosalinities. In: Fischer, G., Wefer, G. (Eds.), Use of Proxies in Paleoceanography: Examples from the South Atlantic. Springer, Berlin, pp. 207–228.

Zaier, A., Beji-Sassi, A., Sassi, S., Moody, R.T.J., 1998. Basin evolution and deposition during the early Paleogene in Tunisia. In: Macgregor, D.S., Moody, R.T.J., Clark-Lowes, D.D. (Eds.), Petroleum Geology of North Africa. Geol. Soc. Lond. Spec. Publ. 132, 375–393.

Zachos, J.C., Arthur, M.A., Thumell, R.C., Williams, D.F., Tappa, E.J., 1985. Stable isotope and trace element geochemistry of carbonate sediments across the Cretaceous/Tertiary boundary at Deep Sea Drilling Project Hole 577, Leg 86. Init. Rep. Deep Sea Drill. Proj. 86, 513–532.

Zachos, J.C., Arthur, M.A., 1986. Paleoceanography of the Cretaceous/tertiary boundary event, inferences from stable isotopic and other data. Paleoceanography 1, 5–26.